Theor Chem Acc (1997) 96:23–30

Theoretical Chemistry Accounts

Original articles

Approximation of the molecular electrostatic potential in a gaussian density functional method

M. Leboeuf, A.M. Köster* and D.R. Salahub

Département de chimie, Université de Montréal, C.P. 6128 Succ. Centre-ville, Montréal, QC, Canada H3C 3J7
CERCA-Centre de Recherche en Calcul Appliqué 5160, Boul. Décarie, Bureau 400, Montréal, Québec, Canada H3X 2H9

Received: 5 July 1996 / Accepted: 12 November, 1996

Abstract. The recently developed Asymptotic Density Model (ADM) [6, 9] is here implemented in the density functional framework using the program deMon-KS [13]. While the original implementation divided the atoms into a core shell and a valence shell, the present version allows for an arbitrary number of shells making it therefore more flexible and, as shown with benzene, potentially more accurate. Moreover, since this method is derived through Poisson's equation, an expression for the electronic charge density is also obtained. However, the present discussion will restrict itself to the electrostatic potential. Finally, even though this method requires parametrization, it is shown that the parameters obtained for homonuclear diatomic species, and used as is in molecular calculations, yield satisfactory results. Indeed, the ADM reproduces almost all basic features of the MEP for all molecules presented here, (water, ammonia, ethylene, acetylene, hydrogen cyanide, carbon monoxide, benzene, nitrous acid).

Key words: Density functional theory – Electrostatic potential – Multipole expansion

Introduction

The molecular electrostatic potential (MEP) has proven to be a valuable property in many areas of chemistry [1]. The topography of the MEP has been used to identify important features of the electronic structure of molecules labelled as lone pairs, σ and π bonds, and so on, [2, 3]. Additionally, insight into the reactivity of molecules can be gleaned from the MEP. For example, MEP maps have been used to determine the reactivity of organic compounds towards electrophilic species [1]. Furthermore, long range interactions being largely electrostatic in nature, for example in molecular recognition processes [4], the MEP provides essential enlightenment. Solvation effects can also be mimicked by the MEP, as in the reaction field model of Tomasi [5], which requires the computation of the MEP on the surface of a cavity.

This quantity may be computed quantum-mechanically, but one is then restricted to relatively small molecules because of the large cost of such calculations for systems of even moderate size, if the values of the MEP are required at a large number of points. In order to handle larger systems, an approximate scheme is therefore necessary. Traditionally, the multipole expansion (ME) has been used. However, the errors of the ME grow as one leaves the long range region and enters the important van der Waals region, closer to the nuclei. Recently, Köster *et al.* have developed a new approximate scheme, the Asymptotic Density Model (ADM) [6], which yields a dramatically improved behavior of the MEP over the ME, and at the same time retains its computational efficiency. In this model, Poisson's equation (eq. (1)) is solved by partitioning the molecular electronic density into atomic densities, assuming these are monotonically decreasing functions of **r** [7] in a piecewise exponential fashion, thereby reflecting the shell structure of atoms [8]. Srebrenik, Weinstein and Pauncz [9] have already done similar work. However, their model constitutes more an approximate solution to Poisson's equation than an approximation to the MEP itself or, as is the starting point of the ADM, to the electronic density. The ADM has already been successfully implemented in the HF [6] and INDO [10] methodologies. In this paper, we present an improved implementation of the ADM in the *linear combination of gaussian type orbital-density fuctional* (LCGTO-DF) framework, using water, ammonia, ethylene, acetylene, hydrogen cyanide, carbon monoxide, benzene and nitrous acid as examples.

The asymptotic density model

Instead of attempting to construct directly an approximation for the MEP, one can begin by approximating the charge density of the system and then generate the MEP from Poisson's equation

* *Present address*: Theoretische Chemie, Universität Hannover, Am Kleinen Felde 30, 30167 Hannover, Germany
Correspondence to: D.R. Salahub

$$\nabla^2 U(\mathbf{r}) = -4\pi\rho(\mathbf{r}) \tag{1}$$

$U(\mathbf{r})$ and $\rho(\mathbf{r})$ being respectively the MEP and total charge density. Since the nuclear contribution to the MEP is already known in a simple analytic form, the total MEP can be divided into a nuclear and an electronic part

$$U_{total}(\mathbf{r}) = U_{elec}(\mathbf{r}) + U_{nuc}(\mathbf{r}), \quad U_{nuc}(\mathbf{r}) = \sum_A \frac{Z_A}{|\mathbf{R}_A - \mathbf{r}|} \tag{2}$$

where Z_A and $\mathbf{R}_A$ are the charge and position of atom A. All the effort is therefore put into determining U_{elec} *i.e.* ρ_{elec}.

In the original ADM scheme [6], the authors proposed to express this electronic density as a sum of atomic densities which were in turn sums of core, valence and polarisation terms

$$\rho_{elec}(\mathbf{r}) = \sum_A \rho^A_{elec}(\mathbf{r}_A) \tag{3}$$

$$\rho^A_{elec}(\mathbf{r}_A) = \rho^A_{elec,core}(\mathbf{r}_A) + \rho^A_{elec,val}(\mathbf{r}_A) + \rho^A_{elec,pol}(\mathbf{r}_A) \tag{4}$$

This scheme is suitable for all-electron split valence basis sets for first row atoms (Li-Ne) and valence electron basis sets as used in the INDO methodology. However, to be able to study heavier elements and use larger basis sets, a more general scheme is needed. We, therefore, propose here a more flexible approach in which the atomic densities, ρ^A_{elec}, (hereafter simply called ρ^A) are divided into shell densities

$$\rho^A(\mathbf{r}_A) = \sum_S \rho^{A,S}(\mathbf{r}_A) \tag{5}$$

where the summation runs over the number S of shells. In this way, we are not restricted to a fixed number of shells, but could in principle use as many shells as desired. However, in practice the shell structure *i.e.* the value of S in eq. (5) is dictated by the shell structure of the basis set employed for the calculation. For example, the popular 6-31G basis would give rise to three terms in the expansion for first row elements.

The atomic shell densities are represented as an expansion in Slater functions:

$$\rho^{A,S}(\mathbf{r}_A) = \sum_{l=0}^{l_{max}} \sum_{m=-l}^{l} d^S_{lm} r_A^l e^{-\zeta^S_{lm} r_A} S_{lm}(\theta_A, \phi_A) \tag{6}$$

where l and m are the azimuthal and magnetic quantum numbers, and where we again deviate from the original ADM by allowing for the possibility of including higher order spherical harmonics. As the reader may have already recognized, this definition of $\rho^{A,S}(\mathbf{r}_A)$ is similar to the auxiliairy basis set approach in DFT [11], except that we have used Slater type functions instead of gaussians.

With this definition for the electronic density, the electronic part of Poisson's equation becomes, for each atom

$$\frac{1}{r_A^2}\frac{\partial}{\partial r_A}\left[r_A^2 \frac{\partial}{\partial r_A} U^A(\mathbf{r}_A)\right] - \frac{\hat{\mathrm{L}}^2}{r_A^2} U^A(\mathbf{r}_A) = -4\pi\rho^A(\mathbf{r}_A) \tag{7}$$

Since the spherical harmonics are eigenfunctions of the $\hat{\mathrm{L}}^2$ operator,

$$\hat{\mathrm{L}}^2 S_{lm} = l(l+1) S_{lm} \tag{8}$$

we can decompose $U^A(\mathbf{r}_A)$ in a similar fashion as $\rho^A(\mathbf{r}_A)$, that is shell contributions which in turn are sums of a radial term multiplied by an angular part

$$U^A(\mathbf{r}_A) = \sum_S U^{A,S}(\mathbf{r}_A) \tag{9}$$

$$U^{A,S}(\mathbf{r}_A) = \sum_{l=0}^{l_{max}} \sum_{m=-l}^{l} U^S_{lm}(r_A) S_{lm}(\theta_A, \phi_A) \tag{10}$$

and we now have to solve a differential equation in r_A only

$$\sum_{l=0}^{l_{max}} \sum_{m=-l}^{l} \frac{1}{r_A^2}\frac{\partial}{\partial r_A}\left[r_A^2 \frac{\partial U^S_{lm}}{\partial r_A}\right] S_{lm} - \frac{l(l+1)}{r_A^2} U^S_{lm} S_{lm} = -4\pi \sum_{l=0}^{l_{max}} \sum_{m=-l}^{l} d^S_{lm} r_A^l e^{-\zeta^S_{lm} r_A} S_{lm} \tag{11}$$

But it has to be solved for every shell. We therefore seek a general solution for any given l, m combination. Starting from the homogeneous solution

$$U^{S,\mathrm{hom.}}_{lm} = A_{lm} r_A^l + \frac{B_{lm}}{r_A^{l+1}} \tag{12}$$

and taking the following special solution of eq. (11)

$$U^{S,\mathrm{spec.}}_{lm} = -4\pi d^S_{lm}\left[\frac{r_A^l}{(\zeta^S_{lm})^2} + 2(l+1)\sum_{k=2}^{2(l+1)} \frac{[2l]!}{[2l-k+2]!}\frac{r_A^{l-k+1}}{(\zeta^S_{lm})^{k+1}}\right] e^{-\zeta^S_{lm} r_A} \tag{13}$$

we construct the general solution

$$U^{S,\mathrm{gen.}}_{lm} = \frac{A_{lm}(\zeta^S_{lm})^2 - 4\pi d^S_{lm} e^{-\zeta^S_{lm} r_A}}{(\zeta^S_{lm})^2} r_A^l + \frac{B_{lm}(\zeta^S_{lm})^{2l+3} - 8\pi(l+1) d^S_{lm}[2l]! e^{-\zeta^S_{lm} r_A}}{r_A^{l+1}(\zeta^S_{lm})^{2l+3}} - \sum_{k=1}^{2l} \frac{8\pi(l+1) d^S_{lm}[2l]!(\zeta^S_{lm})^{2l-k+1} r_A^{2l-k+1} e^{-\zeta^S_{lm} r_A}}{[2l-k+1]! r_A^{l+1}(\zeta^S_{lm})^{2l+3}} \tag{14}$$

To fix A_{lm} and B_{lm}, similar constraints as in the original paper are imposed, which ensure the proper behavior for the MEP both at long distances and at the nucleus, that is

$$\lim_{r_A \to 0} U^S_{lm}(r_A) = \text{constant} \tag{15}$$

$$\lim_{r_A \to \infty} U^S_{lm}(r_A) = 0 \tag{16}$$

We then find

$$A_{lm} = 0 \tag{17}$$

$$B_{lm} = \frac{8\pi(l+1) d^S_{lm}[2l]!}{(\zeta^S_{lm})^{2l+3}} \tag{18}$$

so that

$$U_{lm}^S(0) = \frac{4\pi d_{00}^S}{(\zeta_{00}^S)^2} \tag{19}$$

To determine the expansion coefficients d_{lm}^S, we rely on the fact that at long distances, the ME is valid. Then, eq. (16) can be rewritten as

$$\lim_{r_A\to\infty} U_{lm}^S(r_A) = \frac{4\pi}{2l+1}\frac{q_{lm}^S}{r_A^{l+1}} S_{lm}(\theta_A,\phi_A) \tag{20}$$

from which we get

$$d_{lm}^S = \frac{(\zeta_{lm}^S)^{2l+3}}{[2l+2]!} q_{lm}^S \tag{21}$$

Substituting (17), (18) and (21) in (14), we obtain the final solution for the electronic part of the MEP

$$U_{lm}^S(r_A) = q_{lm}^S \frac{4\pi}{2l+1}\left[\frac{1-e^{-\zeta_{lm}^S r_A}}{r_A^{l+1}} - \sum_{k=1}^{2l}\frac{(\zeta_{lm}^S)^{2l-k+1}}{[2l-k+1]!} r_A^{l-k} e^{-\zeta_{lm}^S r_A}\right] - q_{lm}^S \frac{4\pi}{[2l+2]!}(\zeta_{lm}^S)^{2l+1} r_A^l e^{-\zeta_{lm}^S r_A} \tag{22}$$

where the q_{lm}^S, introduced via eq. (20), are chosen to be the cumulative atomic multipole moments (CAMM's) [12]. They can be thought of as weighting factors that multiply the contributions of the corresponding shells, arising from the representation of the shell densities by Slater functions. In principle, any definition could be used for the q_{lm}^S, but CAMM's have two undeniable advantages: they are invariant with respect to the orientation of the coordinate system, and they yield a potential $U(\mathbf{r})$ more or less independent of the underlying population analysis, by virtue of their cumulative character, even though the CAMM's themselves are not. Moreover, since the model has to be parametrized, any such dependence upon population analysis would tend to be flattened out. Furthermore, the coordinate system invariance removes the problem of having to take care of the orientation of molecules in space. The only quantities left undefined are the ζ_{lm}^S. These are atomic parameters and are obtained by a least squares fitting of the approximate electronic MEP to the quantum-mechanical one (see below).

The above equations represent a computationally efficient method for calculating the MEP, overcoming the major drawback of the ME, as stated earlier. To study the dynamics of systems where the interactions involved are largely dominated by electrostatics or simply to optimize two charge distributions relative to one another, first and second derivatives of the MEP are needed [13]. Moreover, it is sometimes useful to locate critical points of the MEP in order to get more quantitative information [3]. The most efficient methods to perform this task rely again on the availability of derivatives of the MEP [13]. Calculating the derivatives of the MEP from equation (22) is straightforward. Once Poisson's equation is solved, we have an expression for $U(\mathbf{r}_A)$ which we can differentiate very easily:

$$\frac{\partial^n}{\partial x_i^n} U_{lm}^S(r_A) = q_{lm}^S \frac{4\pi}{2l+1}\left[\frac{\partial^n}{\partial x_i^n}\left(\frac{1-e^{-\zeta_{lm}^S r_A}}{r_A^{l+1}}\right) - \sum_{k=1}^{2l}\frac{(\zeta_{lm}^S)^{2l-k+1}}{[2l-k+1]!}\frac{\partial^n}{\partial x_i^n}\left(r_A^{l-k}e^{-\zeta_{lm}^S r_A}\right)\right] - q_{lm}^S \frac{4\pi}{[2l+2]!}(\zeta_{lm}^S)^{2l+1}\frac{\partial^n}{\partial x_i^n}\left(r_A^l e^{-\zeta_{lm}^S r_A}\right) \tag{23}$$

where x_i stands for x, y and z, and with first derivatives given by

$$\frac{\partial}{\partial x_i}\frac{1-e^{-\zeta_{lm}^S r_A}}{r_A^{l+1}} = \frac{\zeta_{lm}^S x_i}{r_A^{l+2}e^{\zeta_{lm}^S r_A}} - \frac{((l+1)(1-e^{-\zeta_{lm}^S r_A})x_i)}{r_A^{l+3}} \tag{24}$$

$$\frac{\partial}{\partial x_i} r_A^{l-k} e^{-\zeta_{lm}^S r_A} = \frac{r_A^{l-k-2}x_i(l-k-\zeta_{lm}^S r_A)}{e^{\zeta_{lm}^S r_A}} \tag{25}$$

$$\frac{\partial}{\partial x_i} r_A^l e^{-\zeta_{lm}^S r_A} = \frac{r_A^{l-2}x_i(l-\zeta_{lm}^S r_A)}{e^{\zeta_{lm}^S r_A}} \tag{26}$$

We also note that equations (3–6) represent an approximate scheme to compute the electronic density itself (from which we calculated the MEP in the first place). Hence, one can formulate a consistent scheme to build approximations for Coulomb and exchange-correlation energies.

LCGTO-Kohn-Sham implementation and computational details

We have implemented the ADM in the LCGTO-Kohn-Sham code *deMon-KS*. For a more thorough description of the code, see reference [14]. The DZVP basis set was used [15], which is of similar quality to the HF 6-31G* basis. The quantum mechanical (QM) calculations of the MEP used the Generalized Gradient Approximation (GGA) exchange functional of Perdew and Wang [17] and correlation functional of Perdew [18] in conjunction with the local VWN functional [19]. The needed CAMM's were calculated starting from the Mulliken population analysis [20] of the Kohn-Sham orbitals. As discussed earlier, there is no need to use a more sophisticated population analysis. All geometries are experimental, and come from ref. [16]. The current implementation allows CAMM's up to octupole moments, which corresponds to $l_{max} = 3$ in eq. (6). As will be seen later, this limit is sufficient to achieve convergence. The maximum number of shells is set to seven, and corresponding to $S = 7$ in eq. (5) and to the minimum needed to allow for the parametrization of all atoms up to Rn at the DZVP level.

The least squares fitting procedure to determine the ζ_{lm}^S's in eq. (22) is done independently for each atom, and then refined on the corresponding homonuclear diatomic species along the internuclear axis. It is hoped that the parameters hence obtained will be of general use. Indeed, if the model has to be reparametrized for every system to which it is applied, it then looses practicality.

On the other hand, if the atomic parameters are still valid in molecular calculations, then the model becomes much more universal.

Results

As first examples, figures (1)–(4) show the electronic part of the QM and ADM MEP for all atoms parametrized up to now, that is H, C, N and O, for both the atom and the corresponding diatomic molecule. Table 1 gives values for all ζ^S_{lm} used in the calculations presented here. One sees from those pictures that the ADM does exhibit the proper behavior at the atoms. The quantitative agreement is also very good. Indeed, as we get closer to the nuclei, the discrepency between the ADM and QM MEP increases, but up to a distance of around 1 to 1.5 a.u., i.e. inside the van der Waals region of the molecules, the agreement is very good. For carbon and nitrogen, although the quantitative agreement close to the nuclei worsens slightly, it still remains very good. It is worth noting that the expansion converges very rapidly. As can be seen from the figures, already with charges i.e. one term only in eq. (6), the ADM is almost converged. Adding dipole and quadrupole contributions make little change, except in the case of hydrogen where dipoles still make a significant improvement inside the van der Waals region. In all cases studied, octupole moments had virtually no influence at all, so pictures of the ADM MEP including the octupole terms are not presented.

From the foregoing discussions, it seems as if the ADM really fulfills its goal. But how well does it do for molecular systems? Figures 5 to 12 show 2-dimensional cuts of water, ammonia, acetylene, carbon monoxide, hydrogen cyanide, ethylene, benzene and nitrous acid, respectively. In (a) are the QM MEP and in (b), (c) and (d) are the ADM ones calculated with expansion (6) truncated after $l_{max} = 0$ (charge), 1 (dipoles) and 2

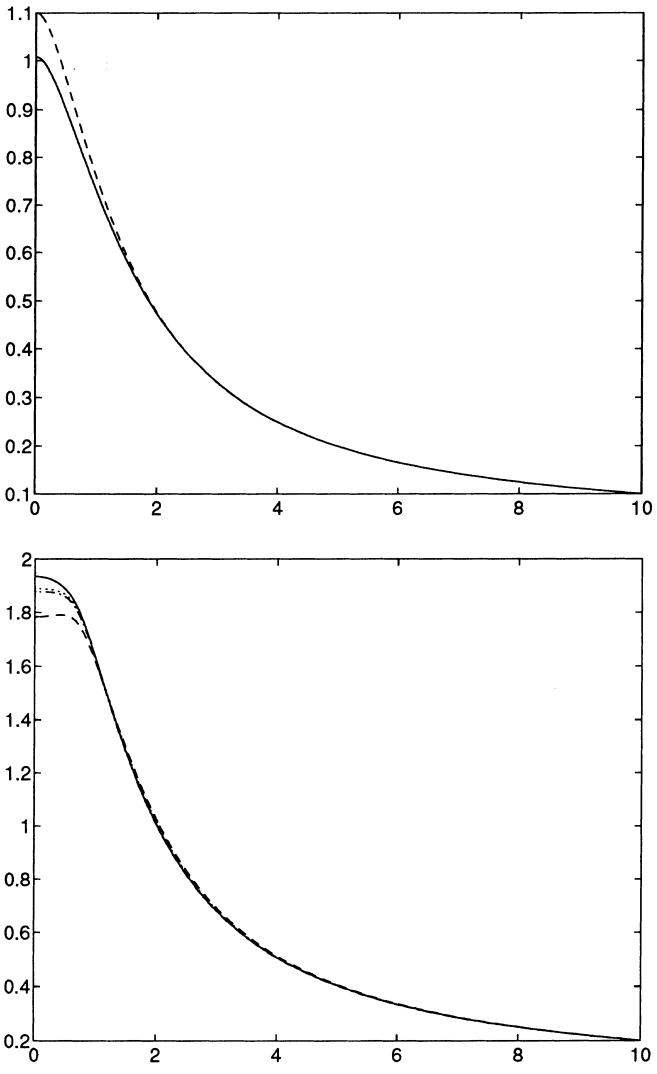

Fig. 1. Electronic MEP of H (top) and H_2 along internuclear axis (bottom) —: QM, – –: ADM/($l_{max} = 0$); –·–: ADM/($l_{max} = 1$); · · · : ADM/($l_{max} = 2$)

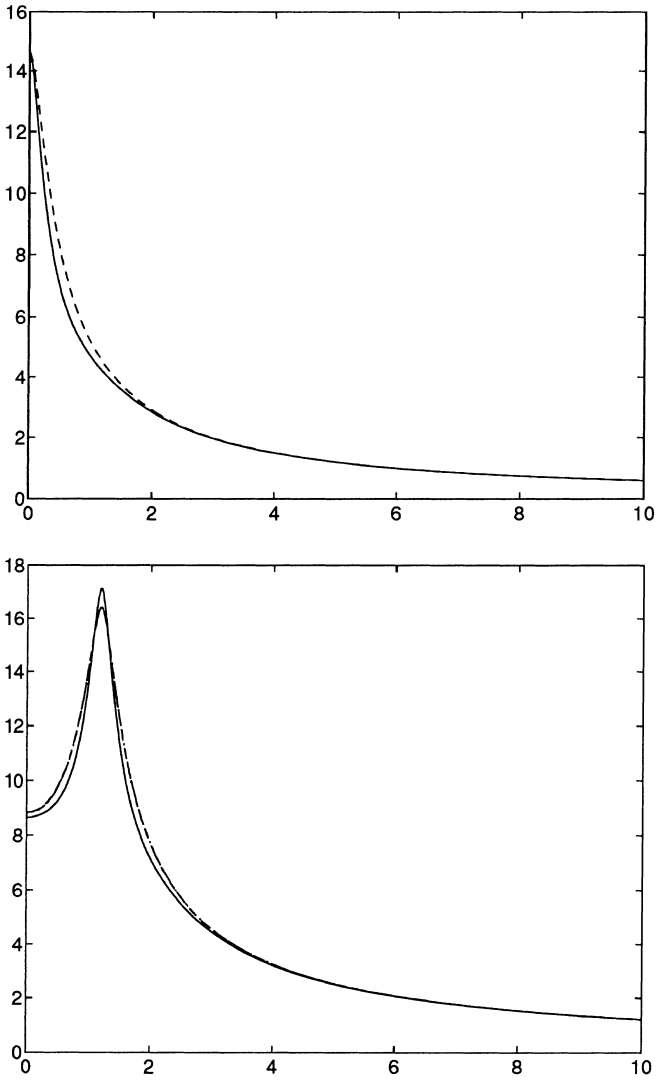

Fig. 2. Electronic MEP of C (top) and C_2 along the half internuclear axis (bottom) —: QM, – –: ADM/($l_{max} = 0$); –·–: ADM/($l_{max} = 1$); · · · : ADM/($l_{max} = 2$)

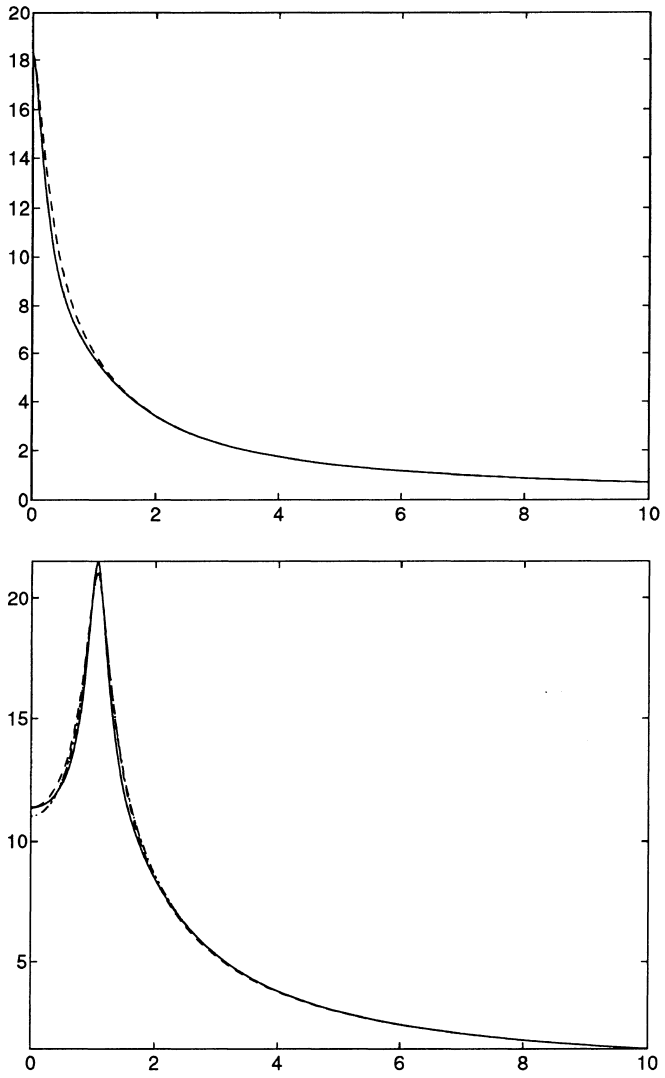

Fig. 3. Electronic MEP of N (top) and N_2 along the half internuclear axis (bottom) —: QM, −−: ADM/($l_{max} = 0$); −·−: ADM/($l_{max} = 1$); ···: ADM/($l_{max} = 2$)

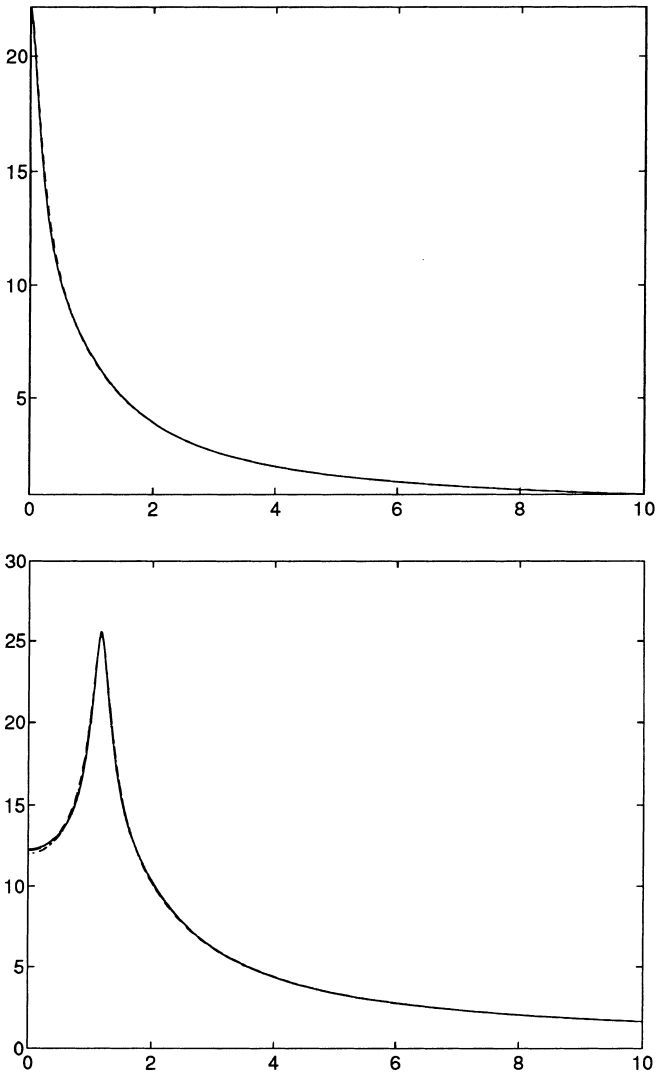

Fig. 4. Electronic MEP of O (top) and O_2 along the half internuclear axis (bottom) —: QM, −−: ADM/($l_{max} = 0$); −·−: ADM/($l_{max} = 1$); ···: ADM/($l_{max} = 2$)

Table 1. ζ^S_{lm} parameters for H,C,N and O.

ζ^S_{lm}	H	C	N	O
ζ^1_{0m}	1,00	0,79	0,86	0,94
ζ^2_{0m}	1,20	1,10	1,00	1,00
ζ^3_{0m}	–	3,60	2,60	1,60
ζ^1_{1m}	2,80	1,00	1,00	1,00
ζ^2_{1m}	1,00	0,50	0,75	1,00
ζ^3_{1m}	–	4,20	3,20	2,20
ζ^1_{2m}	3,00	1,00	1,00	1,00
ζ^2_{2m}	1,00	1,00	1,00	1,00
ζ^3_{2m}	–	1,00	1,00	0,50
ζ^1_{3m}	1,00	1,00	1,00	1,00
ζ^2_{3m}	1,00	1,00	1,00	1,00
ζ^3_{3m}	–	1,00	1,00	1,00

(quadrupoles) respectively, and using the previously diatomic-parametrized ζ^S_{lm}'s. In the first four cases, (H_2O, NH_3, C_2H_2, HCN), the ADM reproduces very well the QM MEP, even showing a very good quantitative agreement with the latter all the way into the van der Waals region. In fact, all major characteristics of the MEP are reproduced by the ADM. For example, the lone pairs of water are easily identifiable by the negative region behind the oxygen, as are the ones of hydrogen cyanide and ammonia. However, the ADM is not able to distinguish between the two lone pairs of water (*cf.* below for nitrous acid) and the inside of the umbrella of ammonia has a more spherical shape than in the QM picture. The triple bond of acetylene is well characterised both by the QM and ADM MEP, with a negative region of toroidal shape around it. As in the atomic (and diatomic) case, the ADM converges very rapidly, terms higher than $l_{max} = 0$ bringing no qualitative changes in the ADM MEP, and the quantitative agreement im-

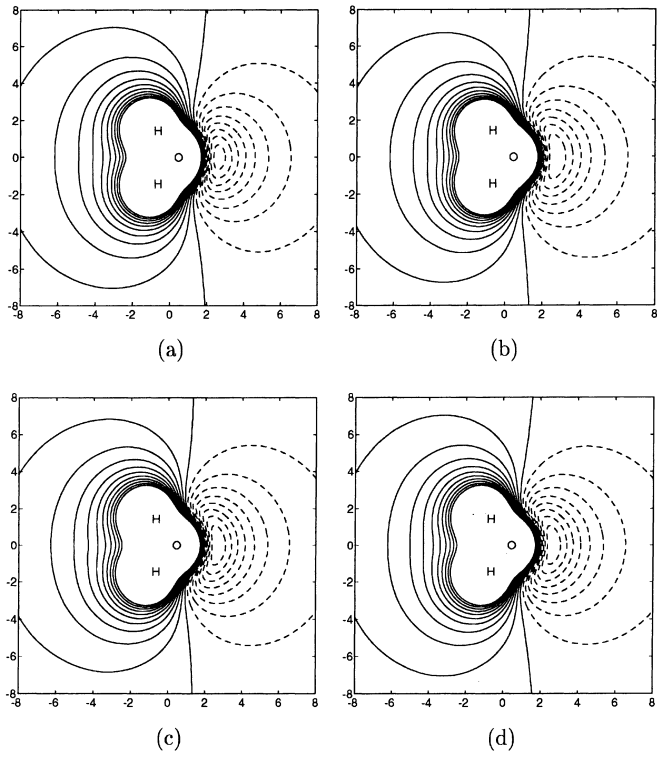

Fig. 5 a-d. Contour map of the MEP of water in the molecular plane. **a** QM, **b** ADM/$l_{max} = 0$, **c** ADM/$l_{max} = 1$, **d** ADM/$l_{max} = 2$. —MEP ≥ 0; ––MEP < 0; each line is at a 0.01 a.u. interval

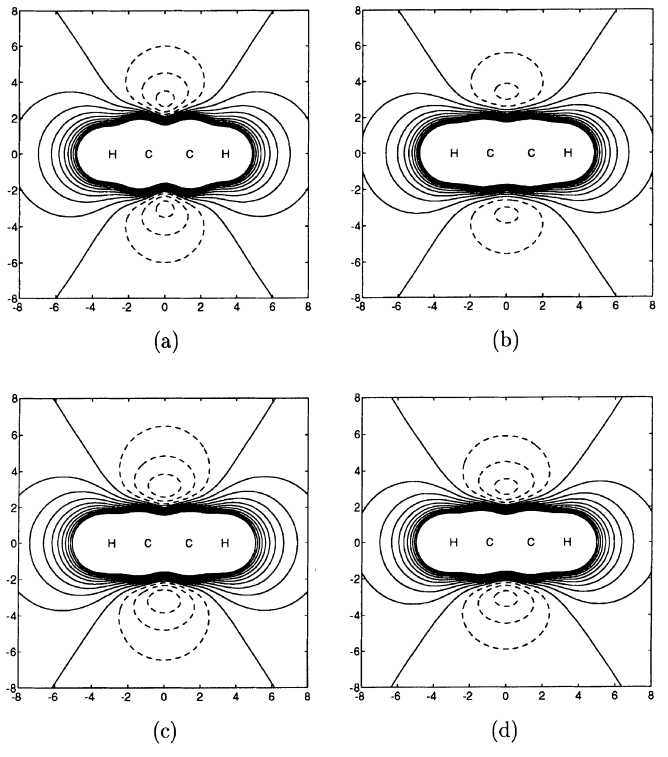

Fig. 7 a-d. Contour map of the MEP of acetylene in a plane containing the molecule. **a** QM, **b** ADM/$l_{max} = 0$, **c** ADM/$l_{max} = 1$, **d** ADM/$l_{max} = 2$. —MEP ≥ 0; ––MEP < 0; each line is at a 0.01 a.u. interval

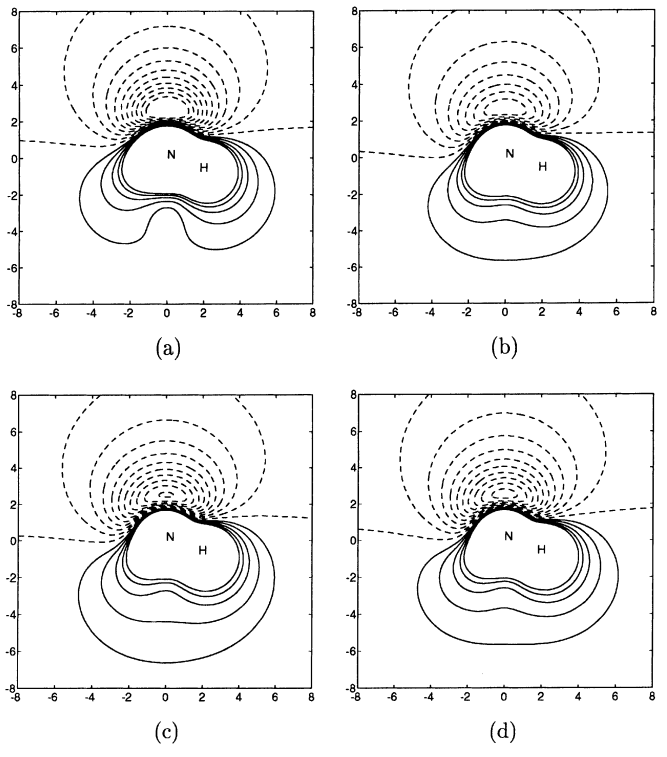

Fig. 6 a-d. Contour map of the MEP of ammonia in one of the $3\sigma_v$ planes. **a** QM, **b** ADM/$l_{max} = 0$, **c** ADM/$l_{max} = 1$, **d** ADM/$l_{max} = 2$. —MEP ≥ 0; ––MEP < 0; each line is at a 0.01 a.u. interval

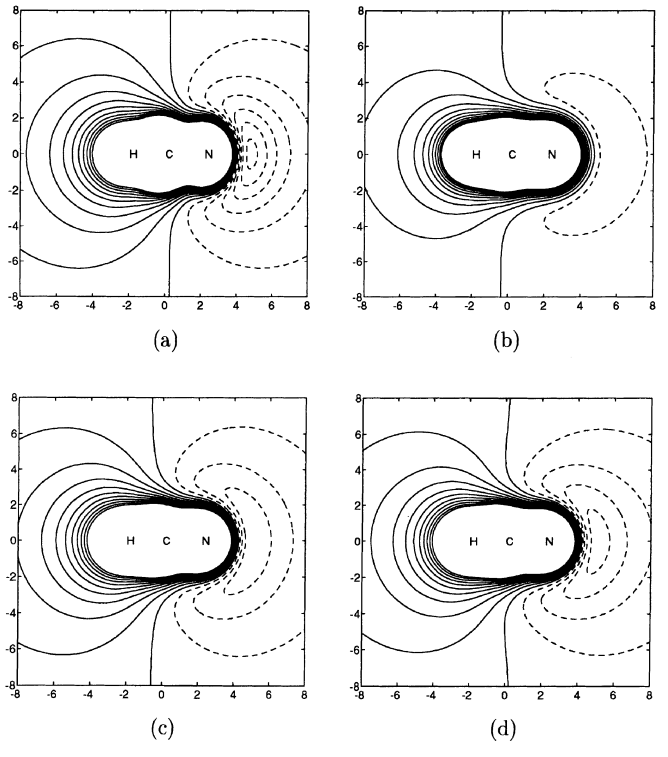

Fig. 8 a-d. Contour map of the MEP of hydrogen cyanide in a plane containing the molecule **a** QM, **b** ADM/$l_{max} = 0$, **c** ADM/$l_{max} = 1$, **d** ADM/$l_{max} = 2$. —MEP ≥ 0; ––MEP < 0; each line is at a 0.01 a.u. interval

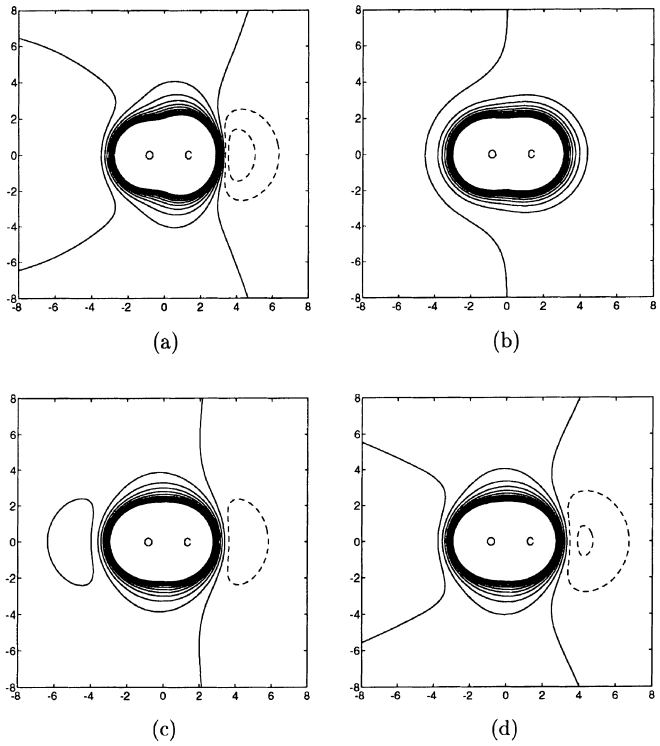

Fig. 9 a-d. Contour map of the MEP of carbon monoxide in a plane containing the molecule. **a** QM, **b** ADM/$l_{max} = 0$, **c** ADM/$l_{max} = 1$, **d** ADM/$l_{max} = 2$. —MEP ≥ 0; ––MEP < 0; each line is at a 0.01 a.u. interval

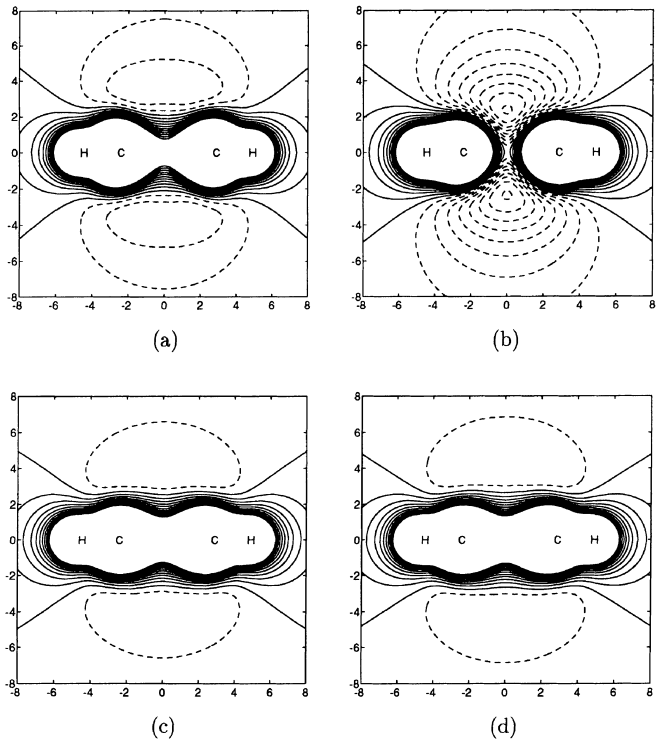

Fig. 10 a-d. Contour map of the MEP of benzene in a plane perpendicular to the molecule and containing two CH bonds. **a** QM, **b** ADM/$l_{max} = 0$, **c** ADM/$l_{max} = 1$, **d** ADM/$l_{max} = 2$. —MEP ≥ 0; ––MEP < 0; each line is at a 0.01 a.u. interval

proving very little. In other words, spherical atomic densities already yield a MEP exhibiting a good topography, non spherical terms being more or less minor corrections. This is in correspondance with Massey's method to calculate the fixed-nuclei static potential part of electron scattering cross sections, which approximates this potential by a linear combination of spherically symetric atom-centered potentials [21].

For the last four molecules, $(CO, C_2H_4, C_6H_6, HNO_2)$, figures 9 to 12, the ADM still gives a very good description of the QM MEP, but second and even third order terms ($l_{max} = 2, 3$ in eq. (6) or (10)), have to be included in order to get as good a description as possible. At the first order of approximation, carbon monoxide (figure 9) is simply wrong, with a positive region behind the oxygen. At the second order, the situation gets better, but it is only at the third that the ADM MEP regains the shape of the QM one. In the case of benzene, it is at $l_{max} = 2$ that the ADM gets a good representation of the MEP, the first order yielding a negative intracyclic region. At the third order, the picture is virtually unchanged. For nitrous acid, as was stated earlier for oxygen, the intraatomic lone pairs are not separated by ADM. However, both oxygens are distinguished by ADM, provided that terms of the second order are included in the calculation. Ethylene constitutes a curious case, showing a good potential at first order that deteriorates at second order, and then becomes good again at the third order of approximation, the best picture being the one at first order.

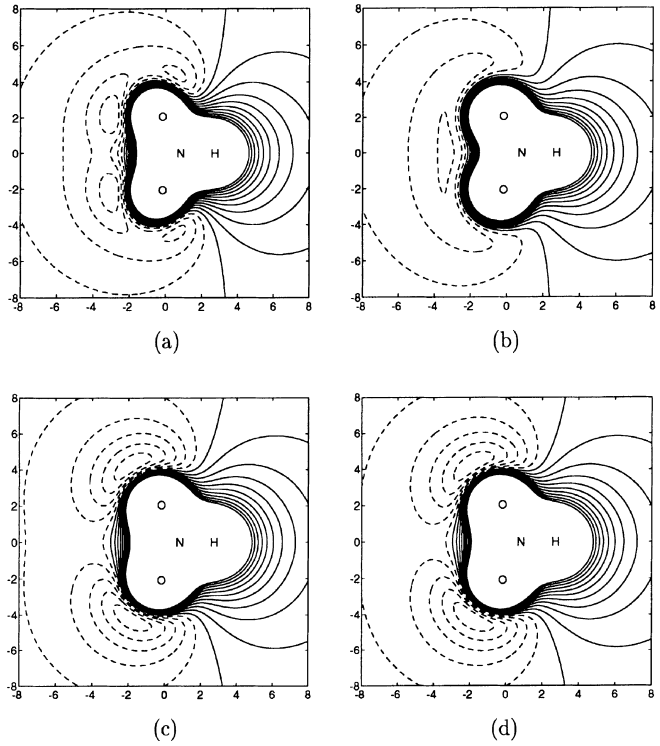

Fig. 11 a-d. Contour map of the MEP of nitrous acid in the molecular plane. **a** QM, **b** ADM/$l_{max} = 0$, **c** ADM/$l_{max} = 1$, **d** ADM/$l_{max} = 2$. —MEP ≥ 0; ––MEP < 0; each line is at a 0.01 a.u. interval

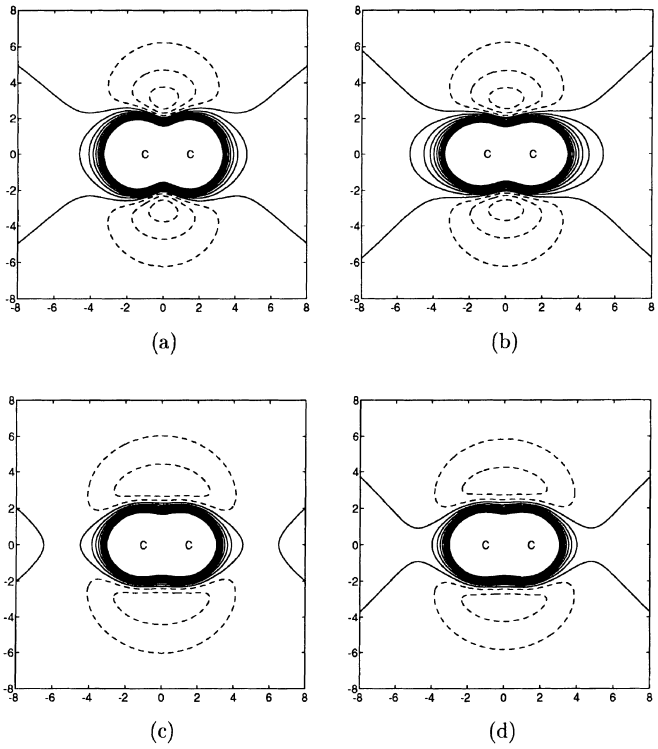

Fig. 12 a-d. Contour map of the MEP of ethylene in a plane perpendicular to the molecule and containing the CC bond. **a** QM, **b** ADM/$l_{max} = 0$, **c** ADM/$l_{max} = 1$, **d** ADM/$l_{max} = 2$. —MEP ≥ 0; ––MEP < 0; each line is at a 0.01 a.u. interval

Conclusion

The Asymptotic Density Model is an excellent alternative to the atomic multipole expansion. Indeed, while having almost as low a computational cost as the latter, it overcomes its major drawback, that is it presents a much improved behavior in the Van der Waals region of molecules. The current implementation, which we feel is better than the original one, seems to improve even further this close range behavior. In fact, for all molecules studied here except for one, HNO_2, all basic features of the quantum-mechanical MEP were reproduced by the ADM, which was not the case for benzene in the original implementation. This means that for applications for which a qualitatively good representation of the MEP is necessary but sufficient i.e. the topography of MEP has to be good while the absolute value need not be as good, e.g. in the visualization of electron transfer reactions [22], the ADM can be preferred over both the QM MEP and ME. The quantitative agreement of the ADM with the QM MEP is also quite good, especially taking into account the fact that the model was parametrized on diatomic homonuclear species, and those parameters used, as is, in all other molecular calculations. Moreover, having derived the ADM through Poisson's equation, we also have an expression for the electronic charge density of the system consistent with the MEP. And both of these expressions are easily and straight forwardly differentiable.

Acknowledgements Financial support from NSERC, Biosym Technologies and Volkswagen Stiftung is gratefully acknowledged.

References

1. Politzer P, Truhlar DG (1984) Chemical Applications of Atomic and Molecular Electrostatic Potentials. Plenum, New York
   Pullman B (1990) Int J Quant Chem Quant Biol Symp 17:81
2. Collard K, Hall GG (1977) Int J Quant Chem 12:623
3. Gadre SR, Kulkarni SA, Shrivastava IH (1992) J Chem Phys 96:5253
   Gadre SR, Shrivastava IH (1991) J Chem Phys 94:4384 Pathak RK, Gadre SR (1990) J Chem Phys 93:1770
4. Rein R (1973) Adv Qant Chem 7:335
5. Miestus S, Scrocco E, Tomasi J (1981) Chem Phys 55:117
   Tomasi J, Persico M (1994) Chem Rev 94:2027
6. Köster AM, Kölle C, Jug K (1993) J Chem Phys 99:1224
7. Weinstein H, Politzer P, Srebrenik S (1975) Theor Chim Acta (Berl) 38:159
8. Wang WP, Parr RG (1977) Phys Rev A 16:891
9. Srebrenik S, Weinstein H, Pauncz P (1973) Chem Phys Lett 20:419
10. Krack M, Köster AM, Jug K J Comp Chem in press
11. Sambe H, Felton RH (1975) J Chem Phys 62:1122
    Dunlap BI, Connolly JWD, Sabin JR (1979) J Chem Phys 71:3396
12. Sokalski WA, Poirier RA (1983) Chem Phys Lett 98:86
    Sokalski WA, Sneddon SF (1991) J Mol Graphics 9:74
13. Fletcher R (1987) Practical Methods of Optimization. J. Wiley & sons, Chichester
14. St-Amant A, Salahub DR (1990) Chem Phys Lett 169:387
    Salahub DR et al. (1991) Gaussian-based Density Functional Methodology, Software and Application. In: Labanowski and Andzelm (ed) Density Functional Methods in Chemistry. Springer, New York
    St-Amant A, Ph.D. thesis (1992) Universitè de Montrèal
15. Godbout N, Salahub DR, Andzelm J, Wimmer E (1992) Can J Chem 70:560
16. Hellwege KH, Hellwege AM (ed) (1979) Numerical Data and Functional Relationships in Science and Technology, Group II, Vol. 7: Structure Data of Free Polyatomic Molecules. Landolt-Börnstein, New Series, Springer, Berlin
    H_2 and O_2 from: K.P. Huber KP, G. Herzberg G (1979) Molecular Spectra and Molecular Structure IV. Constants of Diatomic Molecules. Van Nostrand Reinhold, New York
    HNO_2 from: 1st ref. in [3]
17. Perdew JP, Wang Y (1986) Phys Rev B 33:8800
18. Perdew JP (1986) Phys Rev B 33:8822
19. Vosko SH, Wilk L, Nusair M (1980) Can J Phys 58:1200
20. Mulliken RS (1955) J Chem Phys 23:1833
21. Truhlar DG (1972) Chem Phys Lett 15:486
22. Köster AM, Leboeuf M, Salahub DR (1996) In: Murray J, Sen KD (eds) Theoretical and Computational Chemistry, vol. 3, Elsevier, Amsterdam, p.105